



OPEN ACCESS

EDITED BY

Michail Papafaklis,
Alexandra University Hospital, Greece

REVIEWED BY

Diego Gallo,
Polytechnic University of Turin, Italy
Andrzej Polanczyk,
Main School of Fire Service (SGSP), Poland
Michail Mavrogiannis,
University of Oxford, United Kingdom

*CORRESPONDENCE

Christoph Strecker
✉ christoph.strecker@uniklinik-freiburg.de

[†]These authors have contributed equally to this work and shared first authorship

[†]These authors have contributed equally to this work and shared last authorship

RECEIVED 02 March 2023

ACCEPTED 22 May 2023

PUBLISHED 12 June 2023

CITATION

Strecker C, Kopczak A, Saam T, Sepp D, Hennemuth A, Mayerhofer E, Poli S, Ziemann U, Poppert H, Schindler A and Harloff A (2023) Carotid geometry is independently associated with complicated carotid artery plaques. *Front. Cardiovasc. Med.* 10:1177998. doi: 10.3389/fcvm.2023.1177998

COPYRIGHT

© 2023 Strecker, Kopczak, Saam, Sepp, Hennemuth, Mayerhofer, Poli, Ziemann, Poppert, Schindler and Harloff. This is an open-access article distributed under the terms of the [Creative Commons Attribution License \(CC BY\)](https://creativecommons.org/licenses/by/4.0/). The use, distribution or reproduction in other forums is permitted, provided the original author(s) and the copyright owner(s) are credited and that the original publication in this journal is cited, in accordance with accepted academic practice. No use, distribution or reproduction is permitted which does not comply with these terms.

Carotid geometry is independently associated with complicated carotid artery plaques

Christoph Strecker^{1*†}, Anna Kopczak^{2†}, Tobias Saam³, Dominik Sepp⁴, Anja Hennemuth⁵, Ernst Mayerhofer⁶, Sven Poli⁷, Ulf Ziemann⁷, Holger Poppert⁸, Andreas Schindler^{9†} and Andreas Harloff^{1†}

¹Department of Neurology and Neurophysiology, Medical Center—University of Freiburg, Faculty of Medicine, University of Freiburg, Freiburg, Germany, ²Institute for Stroke and Dementia Research, University Hospital, LMU Munich, Munich, Germany, ³Die Radiologie, Rosenheim, Germany, ⁴Department of Neuroradiology, Klinikum rechts der Isar, Technical University of Munich (TUM), Munich, Germany, ⁵Institute for Imaging Science and Computational Modelling in Cardiovascular Medicine, Charité-Universitätsmedizin Berlin, Berlin, Germany, ⁶Department of Neurology, Massachusetts General Hospital, Boston, MA, United States, ⁷Department of Neurology and Stroke and Hertie Institute for Clinical Brain Research, University of Tübingen, Tübingen, Germany, ⁸Department of Neurology, Helios Klinikum München West, Munich, Germany, ⁹Institute of Neuroradiology, University Hospital, LMU Munich, Munich, Germany

Introduction: Complicated carotid artery plaques (cCAPs) are associated with an increased risk of rupture and subsequent stroke. The geometry of the carotid bifurcation determines the distribution of local hemodynamics and could thus contribute to the development and composition of these plaques. Therefore, we studied the role of carotid bifurcation geometry in the presence of cCAPs.

Methods: We investigated the association of individual vessel geometry with carotid artery plaque types in the Carotid Plaque Imaging in Acute Stroke (CAPIAS) study. After excluding arteries without plaque or with insufficient MRI quality, 354 carotid arteries from 182 patients were analyzed. Individual parameters of carotid geometry [i.e., internal carotid artery (ICA)/common carotid artery (CCA) ratio, bifurcation angle, and tortuosity] were derived from time-of-flight MR images. The lesion types of carotid artery plaques were determined according to the American Heart Association classification of lesions by multi-contrast 3T-MRI. The association between carotid geometry and a cCAP was studied using logistic regression after adjusting for age, sex, wall area, and cardiovascular risk factors.

Results: Low ICA/CCA ratios (OR per SD increase 0.60 [95%CI: 0.42–0.85]; $p = 0.004$) and low bifurcation angles (OR 0.61 [95%CI: 0.42–0.90]; $p = 0.012$) were significantly associated with the presence of cCAPs after adjusting for age, sex, cardiovascular risk factors, and wall area. Tortuosity had no significant association with cCAPs. Only ICA/CCA ratio remained significant in a model containing all three geometric parameters (OR per SD increase 0.65 [95%CI: 0.45–0.94]; $p = 0.023$).

Conclusions: A steep tapering of the ICA relative to the CCA and, to a lesser extent, a low angle of the carotid bifurcation were associated with the presence of cCAPs. Our findings highlight the contribution of bifurcation geometry to plaque vulnerability. Thus, assessment of carotid geometry could be helpful in identifying patients at risk of cCAPs.

KEYWORDS

carotid artery, atherosclerosis, carotid geometry, complicated plaque, magnetic resonance imaging, multicontrast plaque imaging

Introduction

Complicated carotid artery plaques, i.e., American Heart Association lesion type (AHA-LT) VI carotid artery plaques (1–3), are associated with an increased risk of future cerebrovascular events as recently demonstrated in the Carotid Plaque Imaging in Acute Stroke (CAPIAS) study (4). Furthermore, such atheromas were three times more frequent ipsilateral to the side of the symptomatic compared with the asymptomatic hemisphere in patients with acute cryptogenic stroke, underlining the embolic potential of these atheromas (5). Since vascular risk factors affect both carotid arteries similarly, there must be other factors that determine unilateral atheroprotection toward a complicated plaque.

For the optimal prevention of ischemic stroke, it is important to understand why a stable plaque turns into a complicated plaque independent of cardiovascular risk factors and degree of stenosis. Recent studies (6–9) demonstrated that a wide bulb of the ICA, a large carotid bifurcation angle, and low wall shear stress (WSS) are independent predictors of wall thickening in early atherosclerosis. High WSS is associated with plaque instability and rupture by endothelial denudation, fibrous cap thinning, intraplaque hemorrhage, and thrombus formation, thereby turning a stable plaque into a complicated plaque (10, 11). Consistently, Tuenter et al. (12) demonstrated an independent association of intraplaque hemorrhage, the most frequent feature of complicated plaques (2), with high WSS using computational fluid dynamics (CFD) in 79 patients with asymptomatic carotid plaques. Similarly, Zhang et al. showed that WSS was significantly higher in regions adjacent to high-risk than low-risk plaques using 4D flow MRI (13). Moreover, Sadat et al. (14) studied peak stresses within the plaques using *in vivo* MRI in combination with finite-element analysis in each of the 25 patients with acute or recent stroke and carotid stenosis. They asserted that maximum stress was significantly higher in patients with acute symptoms than that in patients with symptoms weeks ago, even in a lower degree of internal carotid artery (ICA) stenosis, indicating that mechanical forces of blood flow can form complicated plaques.

Measuring carotid WSS or plaque stress could be useful to identify patients at risk of plaque rupture prior to the stroke. However, these methods are not suited for clinical routine due to the time-consuming techniques such as 4D flow MRI or CFD requiring complex data analyses. By contrast, vascular geometry is an “easier-to-measure” surrogate of such hemodynamics because geometry shapes the flow (15). Thus, recent studies proposed that carotid geometry assessed by CT or MR angiography may serve as a surrogate parameter for critical flow in early (6, 8, 16) and advanced (17, 18) stages of atherosclerosis. Accordingly, Jiang et al. (17) demonstrated an independent association of carotid geometry, i.e., a smaller lumen expansion at the carotid bifurcation, with vulnerable plaques in 501 carotid arteries of 501 patients in the cross-sectional Chinese Atherosclerosis Risk Evaluation II (CARE II) study.

However, the study of Jiang et al. (17) did not include carotid arteries with luminal stenosis, and a similar study on Caucasians,

who show differences in the distribution of carotid atherosclerosis and the incidence of complicated carotid artery plaques (19) compared to Asians, has not yet been performed. Thus, we investigated the interrelation of ICA/common carotid artery (CCA) ratio, bifurcation angle, and tortuosity with the incidence of complicated carotid artery plaques (cCAPs) based on MRI data in a larger multicenter study of Caucasians with acute ischemic stroke.

Methods

Study population

We analyzed a subset of the Carotid Plaque Imaging in Acute Stroke (CAPIAS) study (ClinicalTrials.gov: NCT01284933) that prospectively recruited patients with acute ischemic stroke in the territory of one carotid artery and unilateral or bilateral carotid artery plaques with a plaque thickness of at least 2 mm at any side. Patients with carotid artery stenosis of $\geq 70\%$, according to NASCET criteria, were excluded. CAPIAS was conducted at four large tertiary stroke centers in Germany: Ludwig Maximilian University Munich, Technical University of Munich, Eberhard Karl University of Tuebingen, and Albert Ludwig University of Freiburg. The study design and inclusion criteria have been published previously (5, 20). The study was approved by the responsible ethics committees, and all participants provided written informed consent.

In our present analysis, we included only carotid arteries with plaques and MRI data with sufficient image quality to assess bifurcation geometry.

Carotid plaque imaging

All participants were examined with a 3-Tesla MRI scanner (Magnetom Verio, Skyra, Tim Trio, Prisma or Biograph mMR, Siemens Healthineers, Erlangen, Germany) and a four-channel surface coil (Machnet, Eelde, Netherlands). We obtained time-of-flight (TOF) MR angiographs and axial pre- and postcontrast black-blood T1-, PD-, and T2-weighted sequences with fat suppression and an in-plane resolution of 0.5 mm^2 as described previously (5, 20, 21). Carotid plaque composition was classified according to the modified AHA-LT criteria (22) by two experienced radiologists (TS and AS) blinded to the patients' characteristics (5). Plaques were defined as AHA-LT III if they showed a small eccentric plaque without calcification or a diffuse intimal thickening; AHA-LT IV/V plaques were characterized by a lipid-rich necrotic core surrounded by fibrous tissue with possible calcifications; complicated AHA-LT VI plaques were defined by the presence of a surface defect, intraplaque hemorrhage, or thrombus; and AHA-LT VII plaques were calcified plaques. There were no AHA-LT VIII plaques without lipid core and with possible small calcifications in our study sample (22). Wall area measurements were performed with a custom-designed semiautomatic image analysis tool (CASCADE, University of Washington, Seattle, Washington) (23).

Geometry analysis

TOF data sets were imported into CaroTo, an extension of the MEVISFlow research software (Fraunhofer MEVIS, Bremen, Germany) (24). A centerline was created in each carotid bifurcation after the manual definition of CCA, ICA, and external carotid artery (ECA) as start- and endpoints for centerline computation. Consecutively landmarks including the flow diverter (FD) and ICA were marked (Figures 1A,B). From these landmarks, predefined points were automatically generated on the centerline, indicating the level of each analysis plane. Analysis planes were manually corrected to align perpendicular to the carotid lumen if necessary. This resulted in six cross-sectional planes (Figure 1C): plane 1 on the CCA centerline 1 cm below the flow diverter (CCA1); plane 2 within the carotid bulb between CCA1 and the flow diverter (CCA2); and planes 3–6 along the ICA with the starting point at the FD and oriented perpendicularly to the centerline with a spacing of 3 mm each (ICA1–ICA4). Geometric parameters have been previously described and successfully applied (7, 8, 25) and included (a) ICA/CCA diameter ratio; (b) bifurcation angle (measured by two tangential lines of the first 1 cm of the outer wall of the ECA and ICA starting at the FD); and (c) CCA-ICA tortuosity (ratio of the centerline connection and the direct line of plane CCA1 and plane ICA4; Figure 1C). All analyses of carotid geometry were performed by one experienced rater (LT). In cases of uncertainty, another experienced rater (CS) was consulted for the final decision.

Statistical analysis

Data are presented as mean and standard deviation or median (interquartile range) for continuous variables and as absolute and relative frequencies for categorical variables. Deviations from normality were determined using the Shapiro–Wilk statistic. Depending on data distribution, two-tailed *t*-tests or nonparametric tests were applied as appropriate for continuous variables. To detect statistically significant relations between categorical variables, a chi-square test was applied.

We used mixed-effects logistic regression models to study associations between geometric parameters and cCAPs and account for the clustering of carotid arteries per patient. For regression analysis, the geometric parameters were standardized. We used the following geometric parameters as predictors: ICA/CCA ratio, tortuosity, and bifurcation angle. Models were constructed with patient identifiers as random effects, geometric parameters as fixed-effects independent variables, and cCAP as a dependent variable. In the first step, we adjusted for age, sex, and wall area (model 1), and in the second step, we adjusted additionally for cardiovascular risk factors including hypertension, diabetes mellitus, hypercholesterolemia, and smoking (model 2). Model 3 included model 2 and all three geometric parameters. All models were adjusted for wall area because of the potential interaction of pre-existing atherosclerotic changes with lumen geometry. A two-tailed *p*-value < 0.05 was considered to indicate statistical significance. Odds ratios (ORs) and 95% confidence intervals were calculated. All analyses were performed with IBM SPSS Statistics 28.

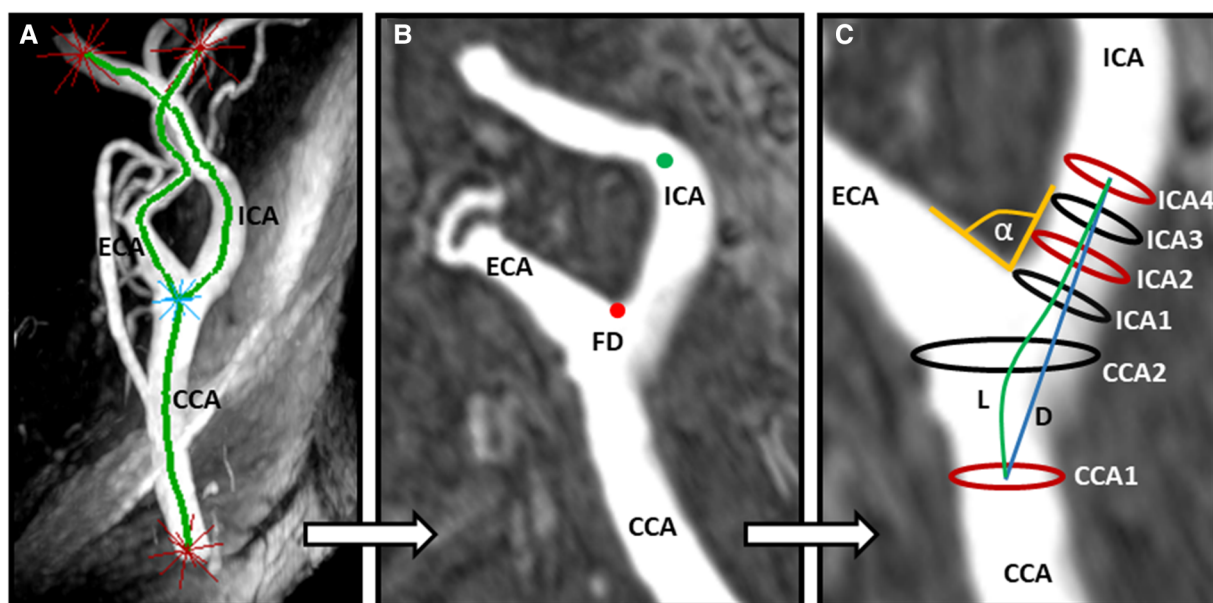


FIGURE 1

Assessment of carotid artery geometry. (A) Computation of a centerline based on time-of-flight (TOF) MR angiography after manually determining starting and end points (labeled as red stars). (B) Manual labeling of the ICA (green dot) and identification of the flow diverter (FD, red dot). (C) Automatic computation of three geometry parameters: α indicates the bifurcation angle; ICA2 and CCA1 represent the maximum diameters for calculation of the ICA/CCA ratio; L and D indicate the CCA–ICA distances along the lumen center (L) and direct connection (D), respectively, for the calculation of carotid tortuosity. CCA, common carotid artery; ICA, internal carotid artery; ECA, external carotid artery.

Results

Study population and baseline characteristics

From 392 carotid arteries ipsilateral and contralateral to the ischemic infarct in 196 patients in the CAPIAS study, 354 carotid arteries (182 patients) were included in the present analysis. Carotid arteries with insufficient image quality/incomplete TOF coverage ($n = 28$) or absence of plaques ($n = 10$) were excluded (Figure 2). Baseline characteristics are provided in Table 1. Complicated plaques were found in 70 carotid arteries (19.8%). Prevalence of noncomplicated plaques was AHA-LT III in 110 (31.3%), AHA-LT IV/V in 68 (19.2%), and AHA-LT VII in 106 (29.9%) carotid arteries. Table 2 compares the geometric parameters and wall areas between carotid arteries with and without complicated plaques.

Association between carotid geometry and plaque composition

The presence of cCAPs, i.e., AHA-LT VI plaques, was significantly associated with a low ICA/CCA ratio (OR per SD increase 0.59 [95%CI: 0.42–0.83]; $p = 0.003$) and a low bifurcation angle (OR per SD increase 0.57 [95%CI: 0.39–0.83]; $p = 0.003$) after adjusting for age, sex, and wall area (model 1). However, such an association was not existent for carotid tortuosity. These findings remained significant for the ICA/CCA ratio (OR per SD increase 0.60 [95% CI: 0.42–0.85]; $p = 0.004$) and bifurcation angle (OR per SD increase 0.61 [95%CI: 0.42–0.90]; $p = 0.012$) after additionally adjusting for cardiovascular risk factors (model 2), indicating that a carotid artery with a smaller lumen expansion of the carotid bulb (i.e., a lower ICA/CCA ratio and thus a steep

TABLE 1 Characteristics of the study cohort.

| Characteristics | N = 182 patients |
|--------------------------------------|-------------------|
| Age, years (\pm SD) | 73.5 (\pm 9.8) |
| Sex, male, n (%) | 128 (70.3) |
| BMI, kg/m ² , (\pm SD) | 26.5 (\pm 3.7) |
| Hypertension, n (%) | 132 (72.5) |
| Diabetes mellitus, n (%) | 38 (20.9) |
| Hypercholesterolemia, n (%) | 59 (32.4) |
| Smoking, n (%) | 100 (54.9) |
| Coronary heart disease, n (%) | 34 (18.7) |
| Stroke/TIA*, n (%) | 34 (18.7) |
| Peripheral artery disease, n (%) | 18 (9.9) |

SD, standard deviation; BMI, body mass index; TIA, transient ischemic attack.
*Prior to the qualifying index stroke.

vessel tapering) in relation to the CCA and a straighter course (lower bifurcation angle) is connected with a higher probability of cCAPs. By integrating all three geometric parameters (model 3), only the ICA/CCA ratio remained significant (OR per SD increase 0.65 [95%CI: 0.45–0.94]; $p = 0.023$), indicating that smaller lumen expansion may be the strongest factor associated with cCAPs. Results of mixed-effects logistic regression analysis regarding geometric parameters (i.e., ICA/CAA ratio, bifurcation angle, and carotid tortuosity) and their association with cCAPs are given in Table 3. The key findings for two carotid arteries with and without a cCAP are illustrated in Figure 3.

Discussion

In the present study, we investigated the association between carotid geometry and a cCAP in 354 carotid arteries of 182 patients who were part of the Carotid Plaque Imaging in Acute Stroke (CAPIAS) study. We were able to demonstrate that a smaller lumen expansion of the internal carotid artery bulb with steep tapering of the vessel into the distal ICA and a low bifurcation angle leading to a straight continuation of carotid blood flow toward the brain (i.e., low ICA/CCA ratios and low bifurcation angles) were independently associated with cCAPs after adjusting for age, sex, wall area, and cardiovascular risk factors. Thus, our findings suggest that the geometry of the carotid bifurcation independently contributes to the risk of cCAPs. Geometry shapes flow, and we believe that local hemodynamics are the underlying drivers of our observations.

Previous investigations

Jiang et al. (17) demonstrated that a smaller luminal expansion of the carotid bifurcation, i.e., a lower “flareA” showed the strongest association with “vulnerable plaques” in Chinese patients. Vulnerable plaques in their study corresponded to AHA-LT VI and IV/V plaques with a large lipid-rich/necrotic core. In our study on Caucasian stroke patients, we used the ICA/CCA ratio, while Jiang et al. used “flareA,” the diameter ratio between distal and more proximal segments in the CCA, in a Chinese cohort. Despite

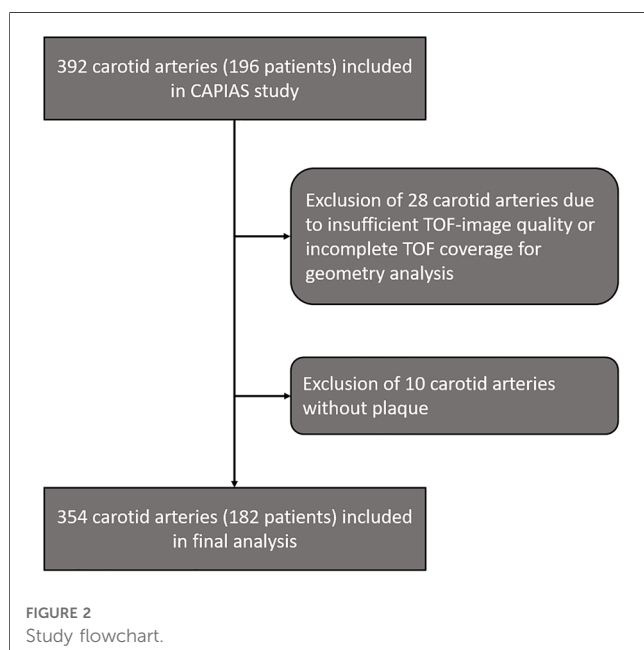


TABLE 2 Geometric and morphological plaque characteristics and wall areas in carotid arteries with complicated carotid artery plaques (cCAPs) defined as American Heart Association lesion type (AHA-LT) VI plaques and non-cCAPs (AHA-LT III, IV/V, VII).

| Characteristics | All carotid arteries | cCAP | non-cCAP | p-value |
|---|----------------------|-----------------|-----------------|---------|
| | (n = 354) | (n = 70) | (n = 284) | |
| ICA/CCA ratio | 0.83 (±0.18) | 0.74 (±0.17) | 0.85 (±0.17) | <0.001 |
| Tortuosity | 1.06 (IQR 0.06) | 1.05 (IQR 0.04) | 1.06 (IQR 0.06) | 0.10 |
| Bifurcation angle (°) | 38.1 (IQR 29.8) | 33.5 (IQR 23.3) | 39.6 (IQR 30.8) | 0.07 |
| Intraplaque hemorrhage, n (%) | 63 (17.8) | 63 (90.0) | NA | NA |
| Juxtaluminal hemorrhage/mural thrombus, n (%) | 51 (14.4) | 51 (72.9) | NA | NA |
| Ruptured fibrous cap, n (%) | 36 (10.2) | 36 (51.4) | NA | NA |
| Wall area (mm ²) | 29.4 (±10.5) | 36.0 (±17.2) | 27.8 (±7.9) | <0.001 |

P-values represent differences between vessels with and without cCAPs. ICA, internal carotid artery; CCA, common carotid artery; NA, not applicable.

TABLE 3 Effects of vascular geometry on the prevalence of cCAPs.

| | cCAP n = 70 | |
|--------------------------|------------------|--------------|
| | OR (95%-CI) | p-value |
| ICA/CCA ratio | | |
| Model 1 | 0.59 (0.42–0.83) | 0.003 |
| Model 2 | 0.60 (0.42–0.85) | 0.004 |
| Model 3 | 0.65 (0.45–0.94) | 0.023 |
| Tortuosity | | |
| Model 1 | 0.76 (0.52–1.11) | 0.155 |
| Model 2 | 0.76 (0.51–1.13) | 0.167 |
| Model 3 | 1.03 (0.65–1.61) | 0.905 |
| Bifurcation angle | | |
| Model 1 | 0.57 (0.39–0.83) | 0.003 |
| Model 2 | 0.61 (0.42–0.90) | 0.012 |
| Model 3 | 0.68 (0.43–1.09) | 0.113 |

OR (95%CI) calculated by mixed-effects logistic regression models clustered per patient. Model 1: adjusted for age, sex, and wall area. Model 2: model 1 additionally adjusted for cardiovascular risk factors (hypertension, diabetes mellitus, hypercholesterolemia, and smoking). Model 3: model 2 and all three geometric parameters.

OR, odds ratio; CI, confidence interval; cCAPs, complicated carotid artery plaques.

these differences, we revealed similar findings; namely, that a smaller luminal expansion in the more distal segments of the carotid artery in relation to the CCA is significantly associated with complicated carotid artery plaques. Thus, our study provides further evidence that individual carotid geometry is associated with plaque composition and plaque instability. In conclusion, there is now evidence from almost 700 stroke patients from Europe and Asia indicating that carotid geometry, especially smaller lumen expansion of the internal carotid artery bulb with steep tapering of the vessel into the distal ICA, is an independent and so far under-recognized predictor for rupture-prone atheroma in the ICA.

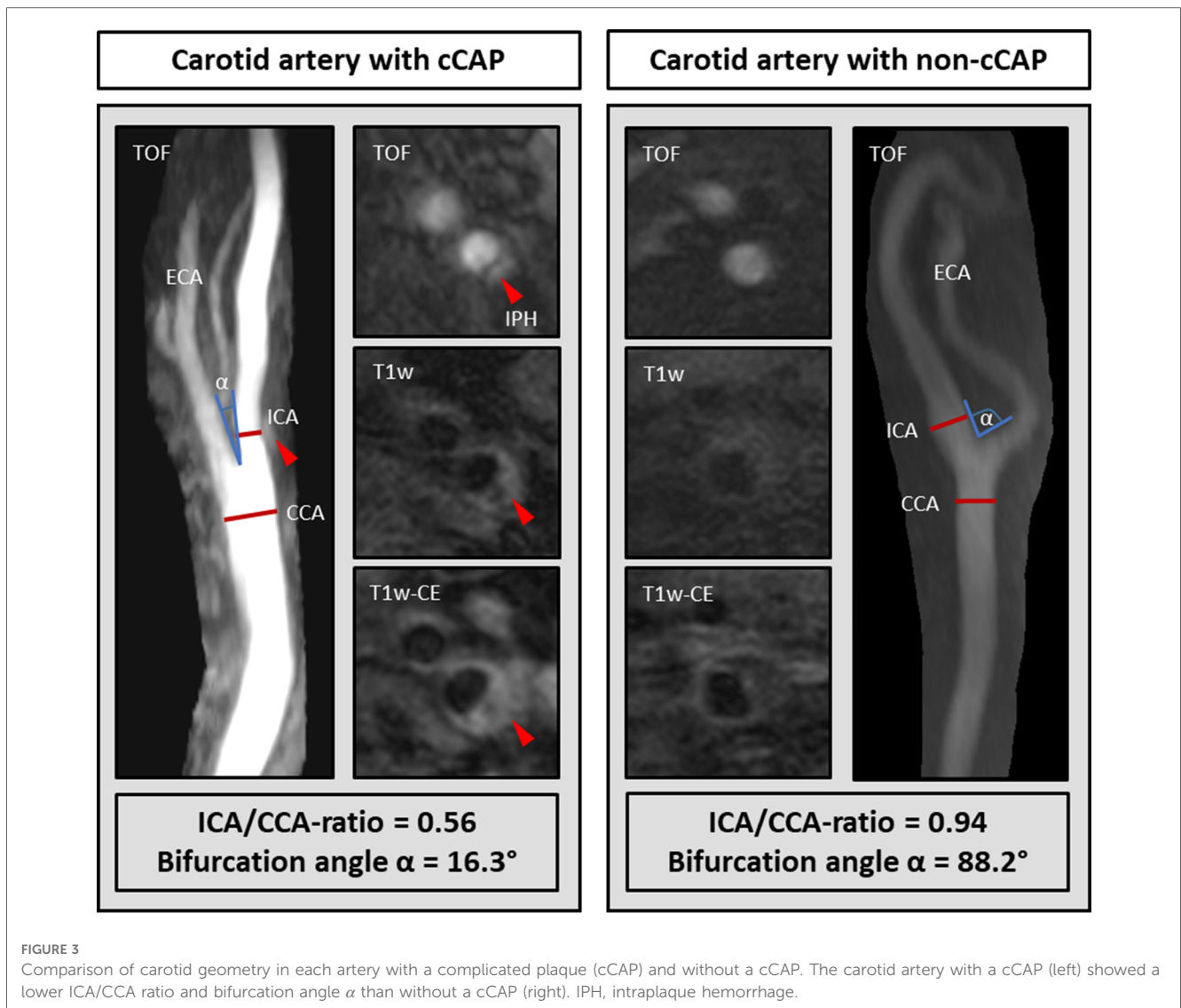
How can the interrelation between geometry and complicated plaques be explained?

A steep tapering of the carotid bulb into the ICA, together with a straight vessel course due to a low carotid bifurcation angle, influences the bloodstream and is likely to result in a

local acceleration of blood flow velocity and pressure. Accordingly, such geometry results in an environment with high local WSS and high pulse pressure acting on the proximal shoulder of the wall and especially on the plaque surface in the case of a significant plaque protrusion. Unfortunately, we cannot provide data on hemodynamics because 4D flow MRI was not part of the protocol, but the interaction of geometry and hemodynamics has been demonstrated in several previous studies (8, 25, 26).

Carotid bifurcations with larger area ratios, i.e., larger ICA/CCA ratios, are more susceptible to low and oscillatory WSS, the so-called disturbed flow, which can be mitigated by a more curved, respectively more tortuous, vessel course (16, 26). Following flow physiology, it is plausible that a smaller lumen expansion, i.e., a steeper tapering of the vessel, reduces disturbed flow and increases WSS accordingly (17). As pointed out, the association between geometry-derived low and oscillating shear stress (8, 9, 26) is well established for the early stages of atherosclerosis. Similarly, there is growing evidence that high WSS plays an important role in the advanced stages of atherosclerosis (12, 27, 28). Combining cellular responses (including plasmin-induced metalloproteinase activity) and high WSS may lead to the degradation of matrix components, smooth muscle cell apoptosis, and reduced matrix synthesis, possibly resulting in intraplaque hemorrhage, fibrous cap thinning, and thrombus formation (10, 27, 29), as shown by Tuenter et al. (12).

As outlined before, carotid geometry also influences mechanical forces of the pulsatile blood flow, especially at the proximal shoulder of plaques and vessel stenosis. These interactions can be measured as plaque stress and tensile stress using finite-element analysis (14, 29–31). It is highly plausible that the steep tapering of the ICA in patients with complicated plaques in our cohort (i.e., low ICA/CCA ratios and low bifurcation angles) leads to high velocities that impinge on the atheroma. Accordingly, high WSS and high pressure, which are the highest in the region of maximal stenosis, act on the wall of the proximal plaque shoulder. On this side, plaque surface and volume deform with each cardiac cycle, predisposing to endothelial leakage, thinning of the fibrous cap, and intraplaque hemorrhage due to shear forces followed by vessel breakage within the plaque (15, 32, 33). This cascade leads to plaque



instability and increases the risk of plaque rupture and stroke. This is supported by the observation of Jiang et al. (17) and Lu et al. (34), who demonstrated that vulnerable plaques occurred more frequently distal to the flow diverter in the ICA, i.e., at the tip or the narrowest section of the funnel.

Limitations

We must consider some limitations of our study. First, we included carotid arteries with mild-to-moderate stenosis. More advanced atherosclerotic changes may potentially alter the geometric parameters. Thus, we corrected for wall area in our models. Even after adjusting for wall area, the association of carotid geometry and complicated plaques remained significant, suggesting that there must be other factors explaining this association beyond wall area and stenosis. In addition to the pathophysiological perspective, including mild-to-moderate stenosis is interesting from a clinical point of view, given that the prevalence of complicated plaques in symptomatic arteries is threefold higher in patients with

cryptogenic stroke (5). Second, we could not interrelate geometry with WSS and plaque type to confirm our pathophysiological explanations since we did not directly measure blood flow; this would have required 4D flow MRI or CFD analysis and should have been done in future studies. Third, our geometry measurements based on 3D TOF images might be hampered due to local irregular blood flow patterns such as flow separation and recirculating flow. Finally, due to the cross-sectional study design, we can only show an association but cannot prove causality. Here, further studies with a longitudinal design are needed.

Conclusions

In this cross-sectional, multicenter study of 354 carotid arteries from 182 patients with acute ischemic stroke, we found a significant association of carotid geometry, i.e., smaller luminal expansion of the ICA and a lower bifurcation angle, with complicated plaques. Our findings might help to identify patients

at increased risk of cCAPs due to their vascular geometry, independent from other predictors such as cardiovascular risk factors and plaque composition. As this plaque type holds a high risk of future strokes, risk stratification and intensified prevention strategies for such patients based on routine CT or MR angiography or ultrasound are of high clinical interest. Furthermore, the results of our study may be valuable for future studies using artificial systems applied for blood flow simulations or engineering tools predicting blood flow hemodynamics (35). To determine the underlying mechanisms of this association, such as the interaction of high wall shear stress or mechanical stress with the plaque, further longitudinal studies using 4D flow MRI or CFD in conjunction with finite-element analysis are required.

Data availability statement

The raw data supporting the conclusions of this article will be made available by the authors without undue reservation.

Ethics statement

The studies involving human participants were reviewed and approved by the Ethics Committee of Ludwig Maximilian University Munich, Technical University of Munich, Eberhard Karl University of Tuebingen, and Albert Ludwig University of Freiburg. The patients/participants provided their written informed consent to participate in this study.

Author contributions

CS recruited participants, performed data analysis, interpreted the data, and drafted the manuscript. AK recruited participants, performed data analysis, and drafted and revised the manuscript. TS performed data analysis and critically revised the manuscript. DS performed data analysis and critically revised the manuscript. AH developed the geometry analysis software and critically revised the manuscript. EM was involved in data interpretation, statistical data analysis, and critical revision of the manuscript. SP recruited participants and critically revised the manuscript. UZ was involved in patient recruitment and critically revised the manuscript. HP recruited participants and critically revised the

manuscript. AS performed data analysis and drafted and revised the manuscript. AH recruited participants, performed data analysis, interpreted the data, and drafted and revised the manuscript. All authors contributed to the article and approved the submitted version.

Funding

This work was funded by the Deutsche Forschungsgemeinschaft (DFG, German Research Foundation) under Germany's Excellence Strategy within the framework of Munich Cluster for Systems Neurology (EXC 2145 SyNergy, ID 390857198). Andreas Harloff was funded by the Berta-Ottenstein-Programme for Advanced Clinician Scientists, Medical Faculty, University of Freiburg and DFG grant HA5399/5-1. Christoph Streckler was funded by DFG grant HA5399/5-1. The article processing charge was funded by the Baden-Wuerttemberg Ministry of Science, Research and Art and the Albert Ludwigs University Freiburg under the Open Access Publishing funding programme.

Acknowledgments

The authors thank Lidia Miguel Telega for performing geometrical analysis.

Conflict of interest

The authors declare that the research was conducted in the absence of any commercial or financial relationships that could be construed as a potential conflict of interest.

Publisher's note

All claims expressed in this article are solely those of the authors and do not necessarily represent those of their affiliated organizations, or those of the publisher, the editors and the reviewers. Any product that may be evaluated in this article, or claim that may be made by its manufacturer, is not guaranteed or endorsed by the publisher.

References

1. Saba L, Saam T, Jager HR, Yuan C, Hatsukami TS, Saloner D, et al. Imaging biomarkers of vulnerable carotid plaques for stroke risk prediction and their potential clinical implications. *Lancet Neurol.* (2019) 18(6):559–72. doi: 10.1016/S1474-4422(19)30035-3
2. Schindler A, Schinner R, Altaf N, Hosseini AA, Simpson RJ, Esposito-Bauer L, et al. Prediction of stroke risk by detection of hemorrhage in carotid plaques: meta-analysis of individual patient data. *JACC Cardiovasc Imaging.* (2020) 13(2 Pt 1):395–406. doi: 10.1016/j.jcmg.2019.03.028
3. Saam T, Underhill HR, Chu B, Takaya N, Cai J, Polissar NL, et al. Prevalence of American Heart Association type VI carotid atherosclerotic lesions identified by magnetic resonance imaging for different levels of stenosis as measured by duplex ultrasound. *J Am Coll Cardiol.* (2008) 51(10):1014–21. doi: 10.1016/j.jacc.2007.10.054
4. Kopczak A, Schindler A, Sepp D, Bayer-Karpinska A, Malik R, Koch ML, et al. Complicated carotid artery plaques and risk of recurrent ischemic stroke or TIA. *J Am Coll Cardiol.* (2022) 79(22):2189–99. doi: 10.1016/j.jacc.2022.03.376
5. Kopczak A, Schindler A, Bayer-Karpinska A, Koch ML, Sepp D, Zeller J, et al. Complicated carotid artery plaques as a cause of cryptogenic stroke. *J Am Coll Cardiol.* (2020) 76(19):2212–22. doi: 10.1016/j.jacc.2020.09.532

6. Bijari PB, Wasserman BA, Steinman DA. Carotid bifurcation geometry is an independent predictor of early wall thickening at the carotid bulb. *Stroke*. (2014) 45(2):473–8. doi: 10.1161/STROKEAHA.113.003454
7. Streckler C, Krafft AJ, Kaufhold L, Hüllebrandt M, Weber S, Ludwig U, et al. Carotid geometry is an independent predictor of wall thickness – a 3D cardiovascular magnetic resonance study in patients with high cardiovascular risk. *J Cardiovasc Magn Reson*. (2020) 22(1):67. doi: 10.1186/s12968-020-00657-5
8. Streckler C, Krafft AJ, Kaufhold L, Hüllebrandt M, Treppner M, Ludwig U, et al. Carotid geometry and wall shear stress independently predict increased wall thickness – a longitudinal 3D MRI study in high-risk patients. *Front Cardiovasc Med*. (2021) 8:723860. doi: 10.3389/fcvm.2021.723860
9. Gallo D, Bijari PB, Morbiducci U, Qiao Y, Xie YJ, Etesami M, et al. Segment-specific associations between local haemodynamic and imaging markers of early atherosclerosis at the carotid artery: an in vivo human study. *J R Soc Interface*. (2018) 15(147). doi: 10.1098/rsif.2018.0352
10. Urschel K, Tauchi M, Achenbach S, Dietel B. Investigation of wall shear stress in cardiovascular research and in clinical practice—from bench to bedside. *Int J Mol Sci*. (2021) 22(11). doi: 10.3390/ijms22115635
11. Eshtehardi P, Brown AJ, Bhargava A, Costopoulos C, Hung OY, Corban MT, et al. High wall shear stress and high-risk plaque: an emerging concept. *Int J Cardiovasc Imaging*. (2017) 33(7):1089–99. doi: 10.1007/s10554-016-1055-1
12. Tuenter A, Selwaness M, Arias Lorza A, Schuurbijs JCH, Speelman L, Cibis M, et al. High shear stress relates to intraplaque haemorrhage in asymptomatic carotid plaques. *Atherosclerosis*. (2016) 251:348–54. doi: 10.1016/j.atherosclerosis.2016.05.018
13. Zhang G, Zhang S, Qin Y, Fang J, Tang X, Li L, et al. Differences in wall shear stress between high-risk and low-risk plaques in patients with moderate carotid artery stenosis: a 4D flow MRI study. *Front Neurosci*. (2021) 15:678358. doi: 10.3389/fnins.2021.678358
14. Sadat U, Li ZY, Young VE, Graves MJ, Boyle JR, Warburton EA, et al. Finite element analysis of vulnerable atherosclerotic plaques: a comparison of mechanical stresses within carotid plaques of acute and recently symptomatic patients with carotid artery disease. *J Neurol Neurosurg Psychiatry*. (2010) 81(3):286–9. doi: 10.1136/jnnp.2009.190363
15. Morbiducci U, Kok AM, Kwak BR, Stone PH, Steinman DA, Wentzel JJ. Atherosclerosis at arterial bifurcations: evidence for the role of haemodynamics and geometry. *Thromb Haemost*. (2016) 115(3):484–92. doi: 10.1160/th15-07-0597
16. Bijari PB, Antiga L, Gallo D, Wasserman BA, Steinman DA. Improved prediction of disturbed flow via hemodynamically-inspired geometric variables. *J Biomech*. (2012) 45(9):1632–7. doi: 10.1016/j.jbiomech.2012.03.030
17. Jiang P, Chen Z, Hippe DS, Watase H, Sun B, Lin R, et al. Association between carotid bifurcation geometry and atherosclerotic plaque vulnerability: a Chinese atherosclerosis risk evaluation study. *Arterioscler Thromb Vasc Biol*. (2020) 40(5):1383–91. doi: 10.1161/ATVBAHA.119.313830
18. Spanos K, Petrocheilou G, Karathanos C, Labropoulos N, Mikhailidis D, Giannoukas A. Carotid bifurcation geometry and atherosclerosis. *Angiology*. (2017) 68(9):757–64. doi: 10.1177/0003319716678741
19. Watase H, Shen M, Sui B, Gao P, Zhang D, Sun J, et al. Differences in atheroma between Caucasian and Asian subjects with anterior stroke: a vessel wall MRI study. *Stroke Vasc Neurol*. (2021) 6(1):25–32. doi: 10.1136/svn-2020-000370
20. Bayer-Karpinska A, Schwarz F, Wollenweber FA, Poppert H, Boeckh-Behrens T, Becker A, et al. The carotid plaque imaging in acute stroke (CAPIAS) study: protocol and initial baseline data. *BMC Neurol*. (2013) 13:201. doi: 10.1186/1471-2377-13-201
21. Saam T, Raya JG, Cyran CC, Bochmann K, Meimarakis G, Dietrich O, et al. High resolution carotid black-blood 3 T MR with parallel imaging and dedicated 4-channel surface coils. *J Cardiovasc Magn Reson*. (2009) 11(1):41. doi: 10.1186/1532-429X-11-41
22. Cai JM, Hatsukami TS, Ferguson MS, Small R, Polissar NL, Yuan C. Classification of human carotid atherosclerotic lesions with in vivo multicontrast magnetic resonance imaging. *Circulation*. (2002) 106(11):1368–73. doi: 10.1161/01.CIR.0000028591.44554.F9
23. Kerwin W, Xu D, Liu F, Saam T, Underhill H, Takaya N, et al. Magnetic resonance imaging of carotid atherosclerosis: plaque analysis. *Top Magn Reson Imaging*. (2007) 18(5):371–8. doi: 10.1097/rmr.0b013e3181598d9d
24. Wehrum T, Kams M, Schroeder L, Drexler J, Hennemuth A, Harloff A. Accelerated analysis of three-dimensional blood flow of the thoracic aorta in stroke patients. *Int J Cardiovasc Imaging*. (2014) 30(8):1571–7. doi: 10.1007/s10554-014-0511-z
25. Markl M, Wegent F, Zech T, Bauer S, Streckler C, Schumacher M, et al. In vivo wall shear stress distribution in the carotid artery: effect of bifurcation geometry, internal carotid artery stenosis, and recanalization therapy. *Circ Cardiovasc Imaging*. (2010) 3(6):647–55. doi: 10.1161/CIRCIMAGING.110.958504
26. Lee SW, Antiga L, Spence JD, Steinman DA. Geometry of the carotid bifurcation predicts its exposure to disturbed flow. *Stroke*. (2008) 39(8):2341–7. doi: 10.1161/STROKEAHA.107.510644
27. Dolan JM, Kolega J, Meng H. High wall shear stress and spatial gradients in vascular pathology: a review. *Ann Biomed Eng*. (2013) 41(7):1411–27. doi: 10.1007/s10439-012-0695-0
28. Groen HC, Gijzen FJ, van der Lugt A, Ferguson MS, Hatsukami TS, van der Steen AF, et al. Plaque rupture in the carotid artery is localized at the high shear stress region: a case report. *Stroke*. (2007) 38(8):2379–81. doi: 10.1161/STROKEAHA.107.484766
29. Slager CJ, Wentzel JJ, Gijzen FJ, Schuurbijs JC, van der Wal AC, van der Steen AF, et al. The role of shear stress in the generation of rupture-prone vulnerable plaques. *Nat Clin Pract Cardiovasc Med*. (2005) 2(8):401–7. doi: 10.1038/ncpcardio0274
30. Costopoulos C, Timmins LH, Huang Y, Hung OY, Molony DS, Brown AJ, et al. Impact of combined plaque structural stress and wall shear stress on coronary plaque progression, regression, and changes in composition. *Eur Heart J*. (2019) 40(18):1411–22. doi: 10.1093/eurheartj/ehz132
31. Costopoulos C, Huang Y, Brown AJ, Calvert PA, Hoole SP, West NEJ, et al. Plaque rupture in coronary atherosclerosis is associated with increased plaque structural stress. *JACC Cardiovasc Imaging*. (2017) 10(12):1472–83. doi: 10.1016/j.jcmg.2017.04.017
32. Gijzen F, van der Giessen A, van der Steen A, Wentzel J. Shear stress and advanced atherosclerosis in human coronary arteries. *J Biomech*. (2013) 46(2):240–7. doi: 10.1016/j.jbiomech.2012.11.006
33. Crombag G, Aizaz M, Schreuder F, Benali F, van Dam-Nolen DHK, Liem MI, et al. Proximal region of carotid atherosclerotic plaque shows more intraplaque hemorrhage: the plaque at risk study. *AJNR Am J Neuroradiol*. (2022) 43(2):265–71. doi: 10.3174/ajnr.A7384
34. Lu M, Cui Y, Peng P, Qiao H, Cai J, Zhao X. Shape and location of carotid atherosclerotic plaque and intraplaque hemorrhage: a high-resolution magnetic resonance imaging study. *J Atheroscler Thromb*. (2019) 26(8):720–7. doi: 10.5551/jat.47449
35. Polanczyk A, Podgorski M, Wozniak T, Stefanczyk L, Strzelecki M. Computational fluid dynamics as an engineering tool for the reconstruction of hemodynamics after carotid artery stenosis operation: a case study. *Medicina (Kaunas)*. (2018) 54(3). doi: 10.3390/medicina54030042